The Impact of Sintering Temperature on the Microstructure and Electrical Characteristics of Varistor Ceramics Containing V_2O_5-doped ZnO-Bi_2O_3-Sb_2O_3 and MnO_2 Additives

D. Umaru and Hassana Mohammed Shuwa

Department of Physics, Faculty of Science, Yobe State University, P.M.B 1144, Kashim Ibrahim Way, Damaturu, Yobe State-Nigeria

**Corresponding author E-mail*: dahiruumaru8@gmail.com

(Received 20 June 2024, Accepted 05 August 2024, Published 20 August 2024)

Abstract

This study explores the enhancement of ZnO varistor ceramics as voltage surge protectors for electronic components by incorporating various metal oxides, including Bi_2O_3, as varistor-forming agents. The investigation focuses on the impact of V_2O_5 doping in ZnO-Bi_2O_3-Sb_2O_3-MnO_2 varistor ceramics to achieve maximum nonlinearity and low leakage current. A mixture of powdered materials (98.1 mol% ZnO, 0.7 mol% Bi_2O_3, 0.3 mol% Sb_2O_3, 0.7 mol% MnO_2, and x mol% V_2O_5) underwent a 24-hour ball milling process, drying, and grounding. The resulting powder was uniaxially pressed into 10 mm diameter, 1 cm thick disks, then sintered at 1240 °C for 4 hours, with a heating and cooling rate of 5°C/min for all compositions. Electrical and microstructural properties were examined for varying V_2O_5 doping levels (x = 0.0 to 0.6 mol%) in ZnO-Bi_2O_3-Sb_2O_3 and MnO_2 varistor ceramics. The maximum barrier height observed was 0.68 eV, corresponding to the highest nonlinearity coefficient 11.25. Minimal leakage current, approximately 1×10^{-4} mA/cm^2, was observed for doping levels of 0, 0.08, 0.20, 0.40, and 0.60 mol%. The highest relative density of the prepared ceramics was 91.31% and 87.23% for ceramics with 0.2 and 0.4 mol% content of doping respectively, this approached the theoretical density of ZnO (5.78 g/cm^3). Microstructural characteristics were examined using SEM attached to EDX. The XRD patterns revealed primary phases of ZnO, with secondary phases including $ZnSb_2O_4$, $Zn_7Sb_2O_{12}$, $MnVO_3$, $BiVO_4$, and $Zn_3(V_4)_2$ polymorphs.

Keywords: Zinc oxide varistor (ZnO); V_2O_5 doped; ZnO Grain boundary; Microstructure; Non-linear electrical properties.

1. Introduction

Zinc oxide varistors (ZnO), are electronic semiconductor ceramics that can protect electronic appliances against unwanted voltage surges transmitted into the electronic components that can cause damage [1]. Varistors are commonly achieved by sintering ZnO oxide powder mixed with some minor metal oxides. Moreover, ZnO varistor materials form a polycrystalline structure after sintering, consisting of semiconductor ZnO grains [2]. The type of metal oxides used is of great importance in ZnO-based varistor fabrication leading to the formation of secondary phases at the grain boundary that trigger the current-voltage characteristics [3]. Generally, the electrical properties, such as nonlinear coefficient, leakage current density, breakdown field, and barrier height, respectively are controlled by the structure or nature of grains and grain boundaries, mostly originating from the segregation of heavy metal oxides such as Bi_2O_3, Pr_6O_{11}, V_2O_5 on ZnO grains or grain boundary [4][5]. The nonlinear I-V characteristics of ZnO-based varistor ceramics are determined from the total number of grain-boundary layers that can be generated during the sintering process, including forming electronic barrier height [6]. Incorporation of minor oxides of MnO_2 in a small percentage can avoid Bi_2O_3 and V_2O_5 evaporation during the sintering process. Also, Sb_2O_3 addition leads to the formation of the $Zn_7Sb_2O_{12}$ spinel phase which reduces the mobility of grain boundaries and regulates ZnO grain growth [8][9][10].

Recent studies have revealed that V_2O_5 alone as a varistor former added on ZnO has the advantage of lowering the sintering temperature but no improvement in the electrical properties promoting grain growth [11]. Hence, there is a need for the incorporation of many additives to increase the nonlinear coefficient of the varistor [12][13][14]. Consequently, combined effects of MnO_2, Pr_6O_{11}, Co_3O_4, and Sb_2O_3 on the ZnO-V_2O_5 contributed to the varistor breakdown potential, which acts from highly resistive to extremely conductive also, the ceramic can be sintered at high temperature of above 1250 ^{O}C [14][15][16].

Although the effect on the performance of V_2O_5 doped ZnO-Bi_2O_3-Sb_2O_3-MnO_2 based varistor ceramics has not been studied symmetrically, there is a report in the literature on the combined ZnO-V_2O_5-MnO_2-Nb_2O_5-Bi_2O_3 based varistor ceramics [17]. Another, combined effect of ZnO-V_2O_5-MnO_2-Nb_2O_5 ceramics was reported [18]. Mn3O4 doping in ZnO-V_2O_5 varistor ceramics was also reported to control ZnO abnormal grain growth [19]. It was reported earlier that incorporating V_2O_5 additives enhances the densification rate of the ZnO materials [20], also the grain-growth rate of the ZnO materials is significantly increased because of V_2O_5 addition.

Mostly, V_2O_5 improves electrical properties particularly the nonlinear current voltage characteristics of ZnO-based varistor ceramic [21]. Another important parameter to be considered is the microstructure properties in which the varistor electrical properties can be determined particularly the current-voltage characteristics of ZnO-based varistor ceramics, the responsible mechanism is grain boundary, better grain boundaries produce an optimum nonlinear current voltage characteristic. Until today, an investigation on the effect of V_2O_5 doped ZnO at 0.5 mol% and low sintering temperature has received attention in many points: degradation behavior, electrical properties, and

microstructure [22][23]. Nevertheless, many problems associated with ZnO-based varistors need to be resolved for commercial purposes. The selected sintering process for specific composition is essential in improving the nonlinear coefficient of ZnO-V_2O_5-based ceramics. As such, it is noteworthy to investigate how a small percentage of V_2O_5-doped ZnO will affect varistor properties for different sintering temperatures. Numerous processing conditions have been established to improve the electrical and microstructural properties of ZnO varistor ceramics [24]. In this work, the impact of sintering temperature and V_2O_5 doping on ZnO-Bi_2O_3-Sb_2O_3-MnO_2-based varistor ceramics has been carefully studied for microstructure and electrical properties.

2. Experimental procedure

High purity of metal oxide powder was carefully selected as the starting material. The powder was obtained from sigma-Aldrich and used in proportion of (98.10) mol% ZnO, 0.2 mol% V_2O_5, 0.7 mol% Bi_2O_3, 0.3 mol% Sb_2O_3, 0.7 mol% MnO_2. The raw materials were mixed via ball-milling with zirconia balls in a polypropylene bottle for 24 h in acetone and a small addition of deionized water to avoid sticking heavy particles like Sb_2O_3. 0.75wt.% poly (vinyl alcohol), 88% hydrolyzed, average M.W.88000 binder was added. The mixture was dried at 110 ^oC for 19 h in an oven and granulated using an agate mortar/pestle, the powder was sieved with 75 micro mesh screens to produce starting powder. The powder was pressed into discs (pellets) of 10 mm diameter, and 1 mm in thickness at a pressure of 50 MPa. The pellets were sintered at 1240 ^oC in air, at intervals for 4 h with a heating and cooling rate of 5^OC/min, and furnace-cooled to room temperature. The shrink-sintered samples were polished to 0.89 mm thickness using SiC paper P1200. Finally, a silver paste was coated on both faces of the pellets and heated at 550 ^oC for 12 min with an electrode area of approximately 0.238 cm^2 to form ohmic contacts.

2.1 Characterization method

The electrical characterization J-I of the samples was recorded at room temperature using a source measure unit (Keithley 2400) to determine (α) of the sintered samples. The varistor voltage (V_{1mA}) was evaluated at a current density between 1-10 $mAcm^{-2}$, and the leakage current density (J_L) was defined as the current density at an applied field of 0.80 V_{1mA} corresponds to J. The α was obtained using the expression below [25][26].

$$\alpha = \frac{(\log J_2 - \log J_1)}{(\log E_2 - \log E_1)} \quad \ldots\ldots (1)$$

With, J_1 = 10 mA/cm^2 and J_2 = 1 mA/cm^2

The morphology of the sintered sample was obtained using a scanning electron microscope (SEM, JEOL JSM-6400), in conjunction with energy dispersive X-ray (EDX) to determine the elements within the composition. The X-ray diffraction pattern of the prepared samples was recorded using (PANalytical X'Pert Pro PW3040/60, Philips). The samples were radiated with Ni-filtered CuKα radiation (λ = 1.5428) within 2θ scan range of 20-80 °C to identify the crystalline phases, the data

were analyzed using X'Pert High Score software. The density of sintered pellets was measured by digital electronic densitometer and the average grain size was calculated by linear intercept method as shown in eqn. (2) [27],[28].

$$d = \frac{1.56L}{MN} \quad \text{..... (2)}$$

Where L is the random line length on the micrograph, M is the magnification of the micrograph and N is the number of grain boundaries intercepted by lines.

3. Result and discussion

3.1 Phase Identification:

The XRD patterns of the sintered varistor ceramics at 1240 °C of different contents of V_2O_5 are shown in **Fig. 1**. The analysis has shown that the V_2O_5 doped ZBSM based varistor ceramics consisted of ZnO-hexagonal structure as the main phase, and V, Sb, and Bi-rich phase as minor secondary phases. For the undoped sample other than the main ZnO phase, $ZnSb_2O_4$ and $Zn_7Sb_2O_{12}$ spinel phases were the only secondary phases identified. However, the phase disappears by doping of V_2O_5 contents. Moreover, secondary phases related to V-species such as $BiVO_4$, $MnVO_3$, and $Zn_3(VO_4)_2$ polymorphs were detected. The formation of $BiVO_4$ is often reported in the combined effect of ZnO–V_2O_5–MnO_2–Nb_2O_5–Bi_2O_3 ceramics [29]. The presence of $Zn_3(VO_4)_2$ is common for all ZnO–V_2O_5-based varistor systems depending on the type of additives, composition, and sintering temperature used [21]. The formation of $Zn_3(VO_4)_2$ was reported by M. Mirzayi, and M.H. Hekmatshoar (2013). The addition of 5 mol % V_2O_5 on ZnO as the main phase acts as a liquid phase sintering at high temperatures enhancing the grain growth of ZnO due to the V_2O_5 additives [30][31]. Another secondary spinel phase related to $Zn_2Sb_7O_{12}$ was observed to inhibit the ZnO grain growth by increasing the V_2O_5 content even though the incremental average grain size may be attributed to the V-rich liquid phase sintering aid.

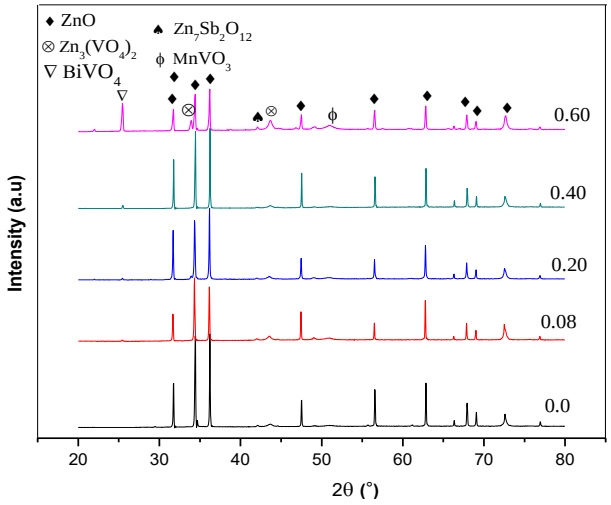

Fig. 1 Shows XRD peaks of the different content of V_2O_5 doped ZBSM sample sintered at 1240 °C.

3.2 Microstructure Characterizations

Fig. 2 (a - e) illustrates the micrographs of SEM of the samples sintered at different contents of V_2O_5. The microstructure was uniformly distributed, except for grain size and shape formation. The initial composition shows a large and defective grain boundary. Significantly, as the concentration of V_2O_5 rises, there is a noticeable increase in the size of the ZnO grains [32] [15], with high reactivity of V–rich phase which is the bed-rock of such exaggeration during the sintering processes [30]. In **Table I** it can be observed that the relative density decreased from 87.23 to 84.53 g/cm^3, this decrease is due to the pores growth and volatility of Bi_2O_3 and V_2O_5 [33] during the sintering processes. The EDX, analysis confirmed the presence of Zn, Mn, V, Bi, and Sb species at the grain boundaries of the prepared ceramics Fig. 3 spectrum 1, 2, and 3 which is a clear indication that the V_2O_5 species have the highest chance to dissolve in ZnO grain. This result was also confirmed by X-ray diffraction analysis (XRD) using (PANalytical X'Pert Pro PW3040/60, Philips). In **Fig. 4** the average grain size decreased from 10.54, 9.22, 7.43, and 7.98 µm with the doping of V_2O_5 than that of 0.0 mol% V_2O_5 of about 11.00 µm which shows poor grain boundaries, this ascribed to the presence of $Zn_7Sb_2O_{12}$ secondary spinel phase [34]. Also, the ceramics exhibit a lower density except for 0.2 mol% with the highest density of 91.31% close to the theoretical density of ZnO.

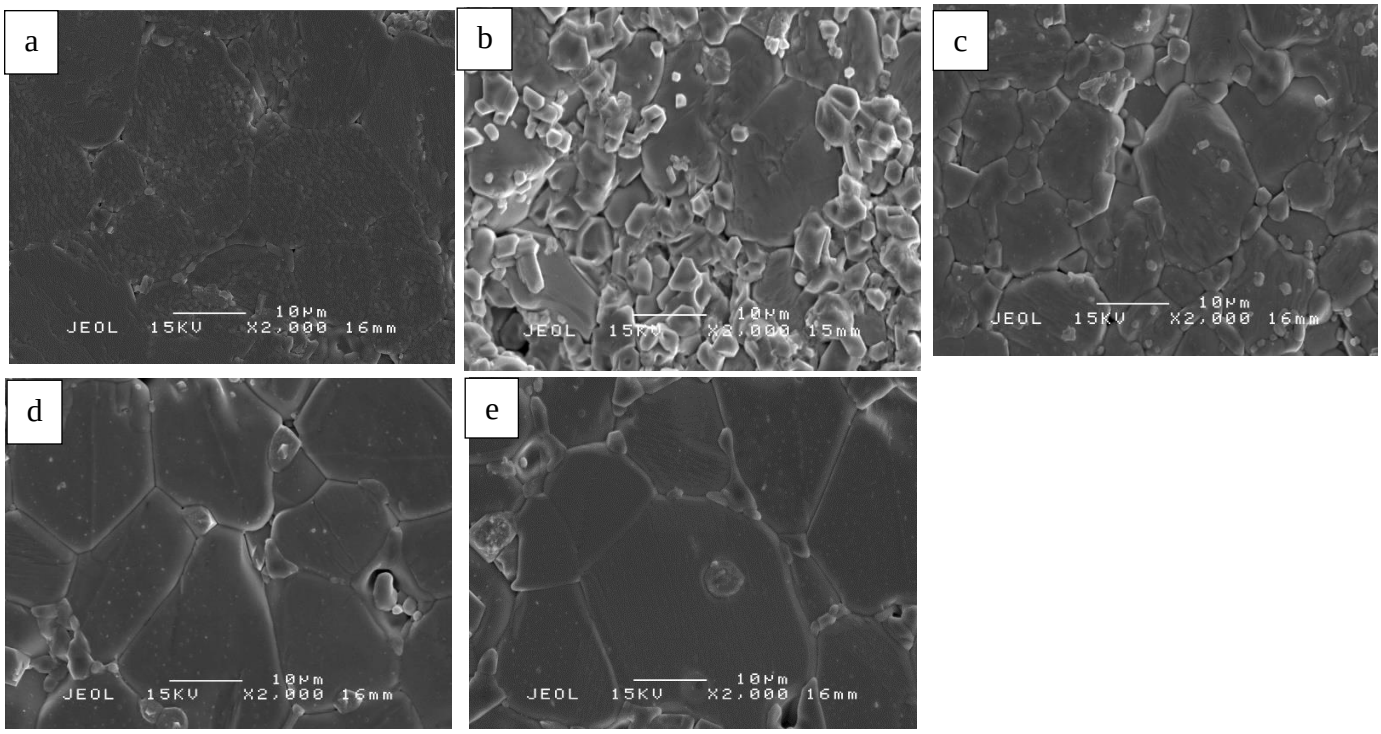

Fig. 2 SEM micrograph of V_2O_5 doped ZBSM sample sintered at 1240 °C, (a) 0.0 mol% (b) 0.08 mol%, and (c) 0.20 mol% (d) 0.40 mol%, and (e) 0.60 mol%.

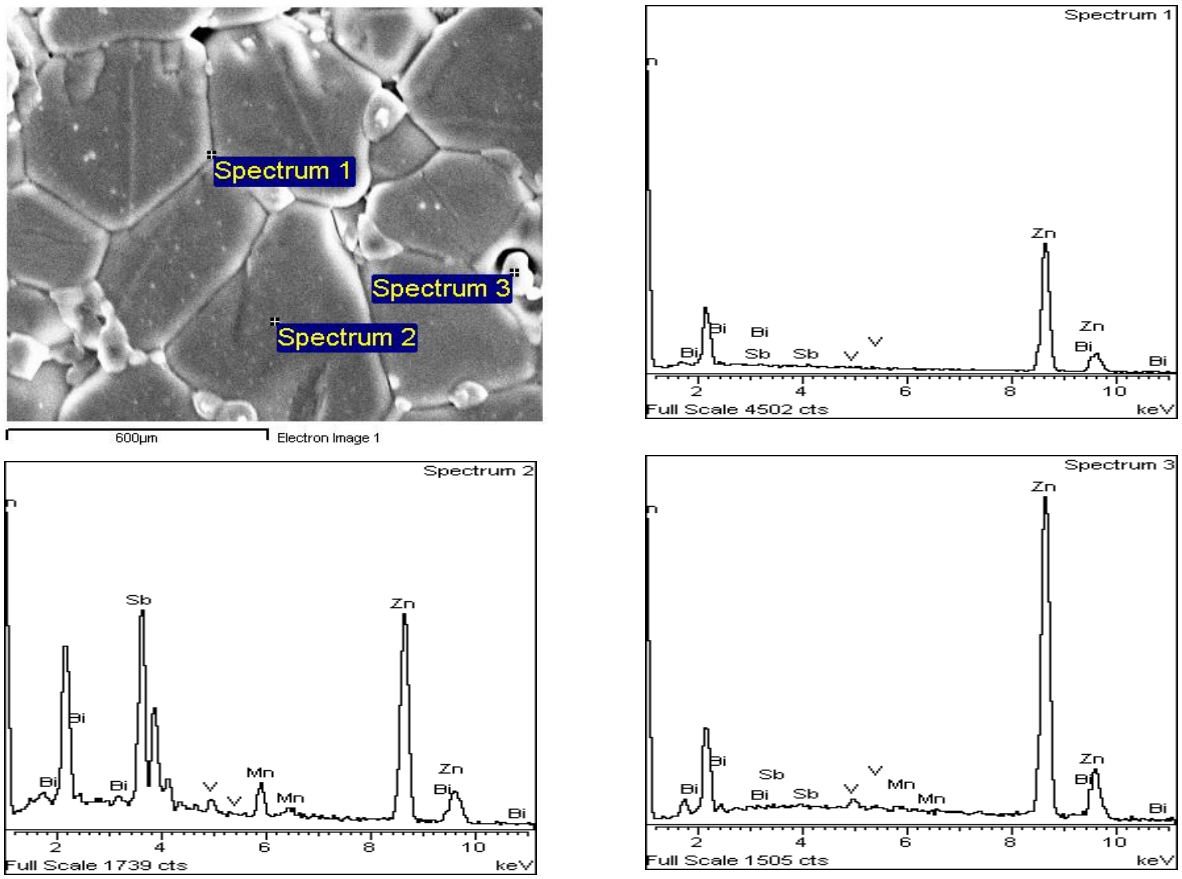

Fig. 3 EDX analysis for 0.4 mol% of V_2O_5 doped ZBSM varistor ceramics sintered at 1240 °C

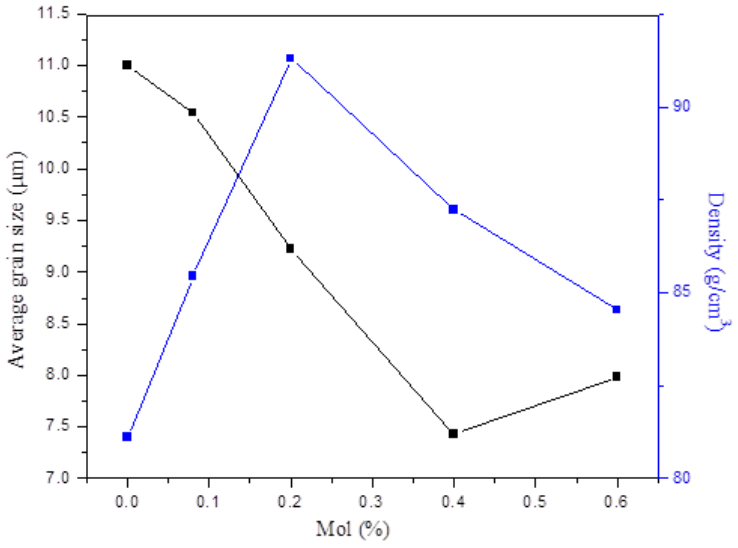

Fig. 4 Illustration of average grain size (µm), and density (g/cm^3), against molar percentage of different content of V_2O_5 sintered at 1240 ^oC.

3.3 Electrical Characterization

The typical E-J characteristics curves and the relation between the non-linear coefficient (α), and molar percentage of the V_2O_5 contents are shown **in Fig. 5a**. The curve behavior is ohmic before the breakdown voltage and becomes nonlinear at a maximum voltage. These are typical characteristics of the varistor-like device. A linear fit was performed to determine the α parameter within the nonlinear region using log J against log E, eq. (1). Sample without V_2O_5 shows a low α value around 4.77 and a maximum leakage current of $4x10^{-4}$ mA/cm^2. It is clearly shown that further incorporating the V_2O_5 content, α value increased to a maximum of 11.25 at 0.2 mol% and the leakage current reduced to a value of $2x10^{-4}$ mA/cm^2. The observed electrical behavior is attributed to the breakdown field of V_2O_5 doped ZBSM-based varistor ceramics, enhanced by 0.2% of V_2O_5 content with a reverse decrease in grain size from 11.00 to 7.98 μm [35]. The relationship between leakage current density, mol%, and α in Fig 4b shows a significant improvement with 0.2 mol% of the V_2O_5 contents which is consistent with average grain size, and percentage density as illustrated in **Table I.**

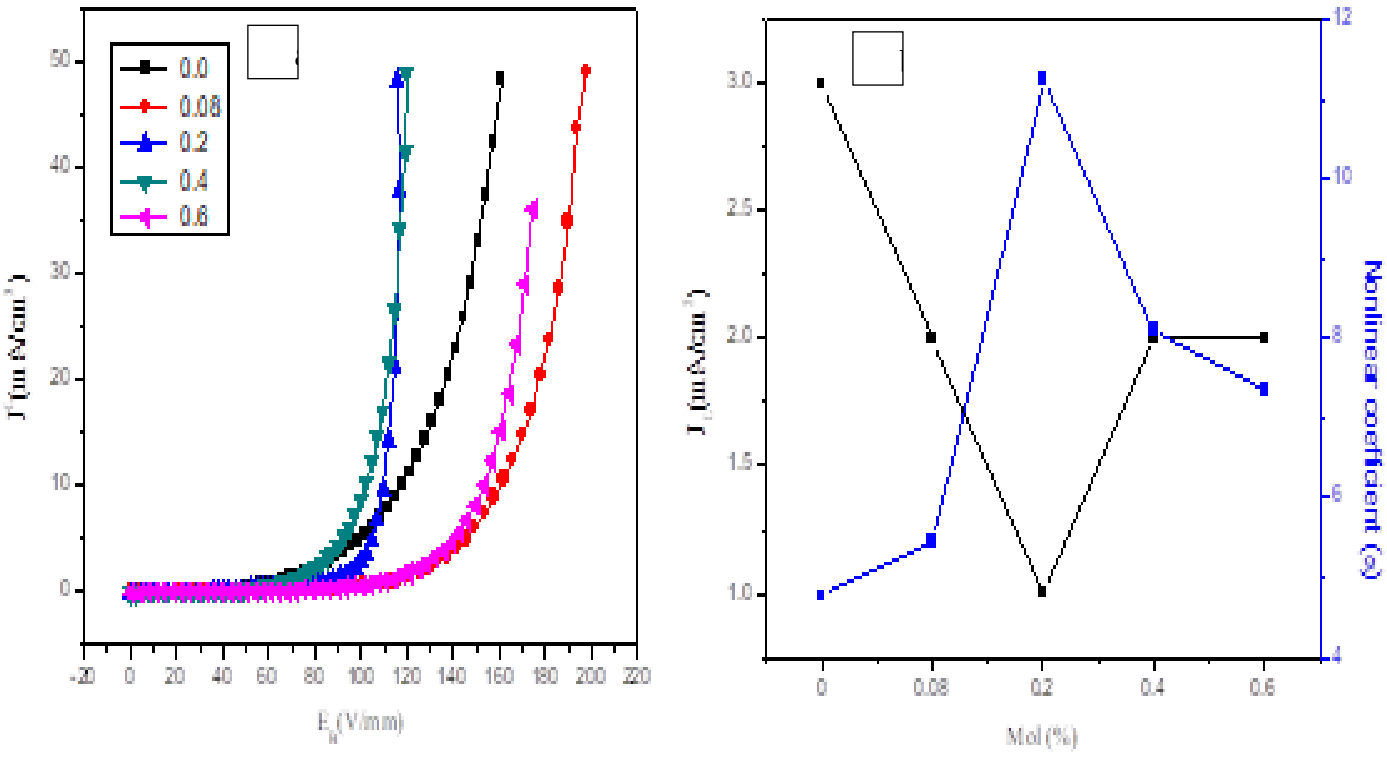

Fig. 5a illustration of J-E characteristic curves of V_2O_5 doped ZBSM samples sintered at 1240 °C, the black curve is 0.0 mol%, the red curve is 0.08 mol%, blue curve is 0.20 mol% and 0.40 mol% is gray, 0.60 mol% pink and **Fig. 5b** shows the relationship between $\boldsymbol{\alpha}$ and percentage mol (%) of V_2O_5 contents.

Table I. Shows electrical and microstructural properties for V_2O_5 doped ZBSM-based varistor ceramics sintered at 1240 ^oC

V_2O_5 content (**mol %**)	**D (μm)**	**ρ (g/cm^3)**	**Φ_B (eV)**	**E_B (V/mm)**	**J_L (mA/cm^2)**	**(α)**
0.0	11.00	81.11	0.60	13.31	4×10^{-4}	4.77
0.08	10.54	85.43	0.90	38.66	3×10^{-4}	5.45
0.20	9.22	91.31	0.68	64.05	2×10^{-4}	11.25
0.40	7.43	87.23	0.81	29.40	3×10^{-4}	8.11
0.60	7.98	84.53	0.90	31.12	3×10^{-4}	7.35

4. Conclusion

The effect of V_2O_5 doped ZBSM-based varistor ceramic ranging from 0.08-0.60 mol% sintered at 1240 ^oC on morphological and electrical properties was carefully studied. The $\boldsymbol{\alpha}$ was observed to increase with the addition of V_2O_5 to an optimum value of 11.25 which was attributed to the observed lowest leakage current $1x10^{-4}$mA/cm^2, and decreased with further incorporation of V_2O_5 content. However, an increase in leakage current 3×10^{-4} mA/cm^2 leads to the drop of $\boldsymbol{\alpha}$ to about 8.11 and 7.35. The excessive doping levels are detrimental, causing a lower voltage $V_{1\ mA}$ around 31.12 V/mm. The density of the sintered ceramics was greatly decreased with increasing V_2O_5 content from 85.43 to 84.53%, except at 0.2 mol% the density was found to be 91.31%, this contributed to a better electrical property, particularly the $\boldsymbol{\alpha}$. The average grain size decreases from 10.54 to 7.98 μm.

Reference

[1] A. Sedky, M. Abu-Abdeen, and A. A. Almulhem, "Nonlinear I–V characteristics in doped ZnO based-ceramic varistor," *Phys. B Condens. Matter*, **388**(1–2), 266–273(2007).

[2] V. O. Varistor, Diao, Chien-chen Chien, Shih-feng Yang, Cheng-fu Chan, Hsien-wu Chen, Ying-chung Chung, and Ho-hua, "The Nonlinear Characteristics of Different Additives Added,"**372**, 493–496(2008).

[3] J. O. Akinnifesi and O. O. Akinwunmi, "Effect of Sintering Temperature on the Microstructure and Electrical Characteristics of Low Clamping Voltage Zinc Oxide-Based Ceramic Varistor," *J. Mater. Sci. Res.*, **4**(3), 40(2015).

[4] M. Dorraj, A. Zakaria, Y. Abdollahi, M. Hashim, and S. Moosavi, "Optimization of Bi_2O_3, TiO_2, and Sb_2O_3 Doped ZnO-Based Low-Voltage Varistor Ceramic to Maximize Nonlinear Electrical Properties," *Sci. World J.*, **2014**, (2014).

[5] C. Leach, Z. Ling, and R. Freer, "The effect of sintering temperature variations on the

development of electrically active interfaces in zinc oxide based varistors," *J. Eur. Ceram. Soc.*, **20**(16), 2759–2765(2000).

[6] H. H. Hng and P. L. Chan, "Effects of MnO_2 doping in V_2O_5-doped ZnO varistor system," *Mater. Chem. Phys.*, **75**(1–3), 61–66(2002).

[7] Anjan Sil, Kiran A., Niranjana A.P., and Kevin M. Knowles, "Sol-gel preparation of Zn-V-Mn-O thin films for low voltage varistor applications, Ceram. Int, 43, 9616–9621(2017).

[8] T. Asokan, G. N. K. Iyengar, and G. R. Nagabhushana, "Studies on microstructure and density of sintered ZnO-based non-linear resistors," *J. Mater. Sci.*, **22**(6), 2229-236(1987).

[9] C. H. Lu, N. Chyi, H. W. Wong, and W. J. Hwang, "Effects of additives and secondary phases on the sintering behavior of zinc oxide-based varistors," *Mater. Chem. Phys.*, vol. **62**(2), 164–168(2000).

[10]M Wang, X Ren, Q Zhou, Z Li, H Yang, H Jiang, Y Yan, X Ruan, W Yu, L Jin, Z Yao, and L Shi, "High improvement of degradation behavior of ZnO varistors under high current surges by appropriate Sb_2O_3 doping," **41**(2020), 436–442(2021).

[11]S. Roy, T. K. Roy, and D. Das, "Grain growth kinetics of Er_2O_3 doped ZnO-V_2O_5 based varistor ceramics," *Ceram. Int.*, **45**(18), 24835–24850(2019).

[12]H. Pfeiffer and K. M. Knowles, "Effects of vanadium and manganese concentrations on the composition, structure and electrical properties of ZnO-rich MnO_2-V_2O_5-ZnO varistors," *J. Eur. Ceram. Soc.*, **24**(6), 1199–1203(2004).

[13]Y. W. Hong and J. H. Kim, "The electrical properties of Mn_3O_4-doped ZnO," *Ceram. Int.*, **30**(7), 1301–1306(2004).

[14]J. H. Ju, H. Wang, and J. W. Xu, "Grain Boundary Characteristics of 0.01 mol%V_2O_5-Doped ZnO-Bi_2O_3-Based Varistor Ceramics," *Adv. Mater. Res.*, **320**(240–243), (2011).

[15]H. H. Hng and K. Y. Tse, "Grain growth of ZnO in binary ZnO-V_2O_5 ceramics," *J. Mater. Sci.*, **38**(11), 2367–2372(2003).

[16]G. Chen, X. Chen, X. Kang, and C. Yuan, "Sintering temperature dependence of varistor properties and impedance spectroscopy behavior in ZnO based varistor ceramics," *J. Mater. Sci. Mater. Electron.*, **26**(4), 2389–2396(2015).

[17]C.-W. Nahm, "Low-temperature sintering effect on varistor properties of ZnO–V_2O_5–MnO_2–Nb_2O_5–Bi_2O_3 ceramics," *Ceram. Int.*, **39(**2), 2117–2121(2013).

[18]C.-W. Nahm, "Effect of sintering process on electrical properties and ageing behavior of ZnO–V_2O_5–MnO_2–Nb_2O_5 varistor ceramics," *J. Mater. Sci. Mater. Electron.*, **23**(2), 457-63(2012).

[19]C. W. Nahm, "Improvement of electrical properties of V_2O_5 modified ZnO ceramics by Mn-doping for varistor applications," *J. Mater. Sci. Mater. Electron.*, **19**(10), 1023–1029(2008).

[20]C. Kuo, C. Chen, and I. Lin, "Microstructure and Nonlinear Properties of Microwave-Sintered ZnO – V_2O_5 Varistors : I , Effect of V_2O_5 Doping," **48**(2942–2948), (1998).

[21]H. H. Hng and P. L. Chan, "Microstructure and current–voltage characteristics of ZnO–V_2O_5–MnO_2 varistor system," *Ceram. Int.*, **30**(7), 1647–1653(2004).

[22]M. Peiteado, J. F. Fernández, and A. C. Caballero, "Varistors based in the ZnO-Bi_2O_3 system: Microstructure control and properties," *J. Eur. Ceram. Soc.*, **27**(13–15), 3867–3872(2007).

[23]H. H. Hng and K. M. Knowles, "Microstructure and Current–Voltage Characteristics of Multicomponent Vanadium-Doped Zinc Oxide Varistors," *J. Am. Ceram. Soc.*, **83**(10), 2455–2462(2000).

[24]C.-S. Chen, C.-T. Kuo, and I.-N. Lin, "Improvement on the degradation of microwave sintered ZnO varistors by postannealing," *J. Mater. Res.*, **13**(6), 1560–1567(2011).

[25]V. V Deshpande, M. M. Patil, and V. Ravi, "Low voltage varistors based on CeO_2," *Ceram. Int.*, **32**(1), 85–87(2006).

[26]M. Science-poland, "The effect of aluminium additive on the electrical properties of ZnO varistors," *Mater. Sci.*, **27**(4), 208–1218(2009).

[27]M. G. M. Sabri, B. Z. Azmi, Z. Rizwan, M. K. Halimah, M. Hashim, and M. H. M. Zaid, "Effect of temperature treatment on the optical characterization of ZnO-Bi_2O_3-TiO_2 varistor ceramics," *Int. J. Phys. Sci.*, **6**(6), 1388–1394(2011).

[28]A. Badev, S. Marinel, R. Heuguet, E. Savary, and D. Agrawal, "Sintering behavior and non-linear properties of ZnO varistors processed in microwave electric and magnetic fields at 2.45GHz," *Acta Mater.*, **61**(20), 7849–7858(2013).

[29]C.-W. Nahm, "Low-temperature sintering effect on varistor properties of ZnO–V_2O_5–MnO_2–Nb_2O_5–Bi_2O_3 ceramics," *Ceram. Int.*, **39**(2), 2117–2121(2013).

[30]M. Mirzayi and M. H. Hekmatshoar, "Effect of V_2O_5 on electrical and microstructural properties of ZnOceramics," *Phys. B Condens. Matter*, **414**(50–55), (2013).

[31]J.-K. Tsai and T.-B. Wu, "Microstructure and nonohmic properties of binary ZnO-V_2O_5 ceramics sintered at 900 °C," *Mater. Lett.*, **26**(3), 199–203(1996).

[32]J. Tian, Y. Wu, H. Tian, Y. Xu, J. Zhao, and P. Lu., "Microstructure and nonlinear electrical properties in Na_2CO_3-ZnO varistor ceramics," *Mater. Sci. Eng. B*, **300**(17084), (2024).

[33]J. Ju, H. Wang, and J. W. Xu, "Grain Boundary Characteristics of 0.01 mol%V_2O_5-Doped ZnO-Bi2O3-Based Varistor Ceramics," *Adv. Mater. Res.*, **320**(240–243), (2011).

[34]J. Li, K. Tang, S. Yang, and D. Zhu, "Effects of Sb_2O_3 on the microstructure and electrical properties of ZnO – Bi_2O_3 -based varistor ceramics fabricated by two-step solid-state reaction route," **47**, 19394–19401(2021).

[35]J. Li, K. Tang, and D. Zhu, "Materials Science in Semiconductor Processing Effect of Ho_2O_3 doping on the microstructure and electrical properties of," **153**(2022), (2023).